HHS Public Access

Author manuscript

Dev Neurobiol. Author manuscript; available in PMC 2017 September 01.

Published in final edited form as:

Dev Neurobiol. 2016 September ; 76(9): 972–982. doi:10.1002/dneu.22369.

Oligodendroglial Defects during Quakingviable Cerebellar Development

Kenneth R Myers[1], **Guanglu Liu**[2], **Yue Feng**[2], and **James Q. Zheng**[1,*]

[1]Departments of Cell Biology and Neurology, Center for Neurodegenerative Diseases, Emory University School of Medicine, Atlanta, GA 30322

[2]Department of Pharmacology, Emory University School of Medicine, Atlanta, GA 30322

Abstract

The selective RNA-binding protein Quaking I (QKI) has previously been implicated in RNA localization and stabilization, alternative splicing, cell proliferation and differentiation. The spontaneously-occurring *quakingviable (qkv)* mutant mouse exhibits a sharply attenuated level of QKI in myelin-producing cells, including oligodendrocytes (OL), due to the loss of an OL-specific promoter. The disruption of QKI in OLs results in severe hypomyelination of the central nervous system, but the underlying cellular mechanisms remain to be fully elucidated. In this study, we used the *qkv* mutant mouse as a model to study myelination defects in the cerebellum. We found that oligodendroglial development and myelination are adversely affected in the cerebellum of *qkv* mice. Specifically, we identified an increase in the total number of oligodendroglial precursor cells in *qkv* cerebella, a substantial portion of which migrated into the grey matter. Furthermore, these mislocalized oligodendroglial precursor cells retained their migratory morphology late into development. Interestingly, a number of these presumptive oligodendrocyte precursors were found at the Purkinje cell layer in *qkv* cerebella, resembling Bergman glia. These findings indicate that QKI is involved in multiple aspects of oligodendroglial development. QKI disruption can impact the cell fate of oligodendrocyte precursor cells, their migration and differentiation, and ultimately myelination in the cerebellum.

Keywords

quakingviable; cerebellum; oligodendroglia; Quaking I; Bergmann glia

Introduction

The ensheathment of axonal fibers by myelin membranes represents a crucial feature in the vertebrate brain that insulates axons for rapid propagation of nerve impulses, as well as to promote axonal survival (Baumann and Pham-Dinh, 2001; Nave, 2010). Loss of the myelin sheath is known to severely disrupt brain function and cause nerve degeneration in a number of neurological disorders (Simons et al., 2014). In the vertebrate central nervous system (CNS), myelination is achieved by oligodendroglia (Emery, 2010). While significant

Correspondence: James Zheng, PhD, Department of Cell Biology, Emory University School of Medicine, 615 Michael Street, Atlanta, GA 30322. Tel: (404) 727-9133. Fax: (404) 727-6256. james.zheng@emory.edu.

progress has been made towards understanding the myelination process and its disruption in human diseases (Emery, 2010), the cellular mechanisms underlying oligodendroglial differentiation and myelination of axons remain to be fully elucidated.

The autosomal recessive *quakingviable* (*qkv*) mutation is a spontaneously occurring deletion encompassing approximately one megabase of chromosome 17 (Sidman et al., 1964; Ebersole et al., 1992). The deleted region contains an enhancer of the *quaking I* gene (*qkI*), which causes reduced expression of QKI specifically in myelinating glia without affecting its expression in other cell types within the CNS (Hardy et al., 1996). Consequently, oligodendrocytes (OLs) in *quakingviable* mice suffer maturation defects and are unable to properly form compact myelin (Chenard and Richard, 2008). Homozygous *quakingviable* (*qkv/qkv*) mice exhibit severe hypomyelination of the central nervous system, as well as rapid tremors beginning at postnatal day 10 (P10) and tonic-clonic seizures during adulthood (Sidman et al., 1964). QKI is a selective RNA-binding protein that governs the post-transcriptional regulation of target mRNAs, including the major constituents of the myelin sheath, myelin basic protein (MBP) and myelin-associated glycoprotein (MAG) (Larocque et al., 2002; Zhao et al., 2010). There are three alternatively-spliced QKI isoforms expressed specifically in glial cells but not neurons, QKI-5, QKI-6, and QKI-7 (Ebersole et al., 1996). While the QKI-6 isoform alone has been shown to be required for proper myelination (Zhao et al., 2006), which exact step(s) of oligodendroglial development is affected by *qkv* mutation remains unclear.

The cerebellum is best known for its unequivocal role in motor control and balance maintenance, as well as involvement in certain cognitive functions of the brain (Buckner, 2013). The cerebellar cortex is highly organized into three distinct layers overlying a core of oligodendrocyte-rich white matter (WM) (Herrup and Kuemerle, 1997). Bordering the WM is the granular layer (GL), which contains granule cells, Golgi cells, and axonal efferents (Purkinje fibers) and afferents (Mossy fibers and climbing fibers) (Sillitoe and Joyner, 2007). Outside of that lies the Purkinje cell layer (PCL) where Purkinje cell neurons and Bergmann glia reside (Sillitoe and Joyner, 2007). The Purkinje cells extend their broad dendritic trees outward into the molecular layer (ML), which is occupied by basket and stellate cells, as well as granule cell axons (parallel fibers) and Bergmann glia fibers (Sillitoe and Joyner, 2007). This stratified organization enables the highly stereotyped neuronal connections that arise between cells from the different layers. While axons in ML are mostly unmyelinated, Purkinje fibers and mossy fibers in GL are highly myelinated. If and how *qkv* mutation affects oligodendroglial development and myelination in the cerebellum has not been closely examined.

While the origins of cerebellar OLs have not been fully understood, the majority of OLs appear to be derived from extra-cerebellar sources, particularly from precursor cells located in the parabasal bands of the mesencephalic neuroepithelium (Mecklenburg et al., 2011). These precursors migrate into the cerebellum through the velum medullare to infiltrate the nascent deep nuclei. From there, they progressively invade the prospective axial white matter outwards towards the pial surface of each folia (Mecklenburg et al., 2011). Once in the cerebellar white matter, the differentiation of OL precursors also proceeds in an inside-out manner from the deep nuclei to the distal white matter and granular layer (Reynolds and

Wilkin, 1988). The mature OLs then extend membrane sheaths as they enwrap axons followed by compaction of mature myelin membrane. Therefore, the cerebellum provides an excellent system to investigate distinct steps of oligodendroglial development leading to the myelination of axonal projections. Importantly, these stages of differentiation can be detected using cell morphology and the expression of specific molecular markers (Baumann and Pham-Dinh, 2001; Zhang, 2001).

In this study, we investigated how the *qkv* mutation affects oligodendroglial development and myelination in the cerebellum using advanced imaging approaches. By utilizing a transgenic mouse line expressing EGFP under the control of the promoter of proteolipid protein (PLP), a major CNS myelin membrane protein (Eng et al., 1968; Mallon et al., 2002), we specifically examined how oligodendroglial localization, migration, and differentiation are affected in *quakingviable* mice. Our results suggest that QKI plays a role in regulating oligodendrocyte migration, their cell fate, differentiation and myelination in the cerebellum.

Methods

Animals

Mice expressing EGFP under the control of the proteolipid protein promoter (PLP-EGFP) and the *quakingviable (qkv/qkv)* mice were described previously (Mallon et al., 2002; Zhao et al., 2006) and were obtained from Jackson Laboratories. *PLP-EGFP; qkv/qkv females* were bred with *w/qkv* males to produce *PLP-EGFP; qkv/qkv* mutants and *PLP-EGFP; w/qkv* littermates. PCR-genotyping was carried out using genomic DNA as previously described (Zhao et al., 2006). Animal care and use was carried out in accordance with NIH guidelines and was approved by the Institutional Animal Care and Use Committee at Emory University.

Organotypic slice cultures and imaging

Cerebellar slice cultures were prepared from postnatal day 7 or 8 (P7 or P8) mouse pups. Mouse pups were anesthetized and decapitated according to institutional guidelines. Brains were removed and cerebella were dissected in cold Hank's Balanced Salt Solution supplemented with 6.5 mg/ml glucose. After removing meninges, sagittal slices were made (400 μm thick) using a McIlwain Tissue Chopper (Ted Pella, Inc). Slices were transferred onto laminin-coated 0.4 μm Millicell cell culture membrane inserts (Millipore) and cultured in Modified Eagle's Medium (MEM) supplemented with 25% horse serum, 25% Hanks Balanced Salt Solution, and 6.5 mg/ml glucose. Imaging was performed on a multi-photon FV1000 laser scanning confocal (Olympus) 24 hours after plating, and every 48 or 72 hours thereafter. Typically, a z-stack comprised of 40–50 optical sections (2 μm step) was acquired using a multi-photon 25X/N.A. 1.05 water immersion objective (XL Plan N, Olympus). Maximal intensity projections of z-stacks were used to generate 2D images, and then 6–8 images were stitched together using ImageJ software (NIH) to visualize entire cerebellar folia.

Immunohistochemistry

Mice were anesthetized with isoflurane and transcardially perfused with 4% paraformaldehyde (PFA) in phosphate-buffered saline (PBS) for 15 minutes. Brains were removed and post-fixed in 4% PFA for 72 hours. Brains were then equilibrated into 30% sucrose and snap frozen in OCT compound (Tissue Tek) for cryosectioning. 30 μm thick free-floating sections were then permeabilized and blocked in PBS containing 20% normal goat serum, 1% bovine serum albumin, 0.3% Triton X-100, and 0.05% Tween-20 for 1 hour. The following primary antibodies were then used to stain sections overnight; anti-Olig2 (Millipore, 1:300), anti-MBP (Covance, 1:1000), anti-Calbindin (Sigma, 1:1000), anti-Ki67 (BD Biosciences, 1:50), and anti-GFAP (Millipore, 1:500). Sections were washed, incubated for 1 hour with anti-rabbit or anti-mouse Alexa-546 secondary antibodies, washed, and mounted on slides with Fluoromount-G (Southern Biotech). Microscopy and imaging were carried out on a Nikon C1 laser-scanning confocal system based on a Nikon inverted microscope (TE300), with a 20X N.A. 0.5 Plan Fluor objective. Maximal intensity projections of z-stacks, typically containing 8–12 optical sections, were used to generate 2D images. Maximal intensity projections of 24–40 adjacent fields were then stitched together using ImageJ to visualize the entire cerebellum. Nikon Elements software was also used to perform semi-automated image analysis from at least three pairs of *qkv/qkv* mice and *w/qkv* littermates. Specifically for cell counting, an automatic intensity threshold was applied to identify individual cells in each cerebellar layer using Elements. The thresholds were then visually inspected to manually select any omitted cells or to separate multiple adjacent cells identified as a single cell, and then converted to a binary. The average number of cells per unit area was calculated for each layer and normalized to the white matter average.

Results

To investigate if and how the quakingviable mutation affects the development of oligodendrocytes and myelination in the cerebellum, we used *qkv/qkv* mice expressing EGFP under the control of the PLP promoter to fluorescently mark OL lineage cells. Specifically, *PLP-EGFP; qkv/qkv females* were bred with *w/qkv* males to produce *PLP-EGFP; qkv/qkv* mutants (hereafter referred to as *qkv/qkv* mice) and non-phenotypic *PLP-EGFP; w/qkv* (hereafter referred to as *w/qkv* mice) littermates. The cerebellum develops postnatally to generate distinct layers of cells with proper synaptic connections. Myelination in the mouse cerebellum also occurs postnatally, beginning during the second week (Foran and Peterson, 1992). We therefore examined the localization of PLP-EGFP+ oligodendroglial cells in the developing cerebellum at P8, P15, and P45, which represent before, during, and after myelination. We first used thin frozen sagittal sections from non-phenotypic *w/qkv* littermate control mice and *qkv/qkv* mice to examine the spatial distribution and morphological changes of PLP-EGFP-expressing cells at these developmental stages. At P8, which is two days prior to the onset of the “quaking” phenotype in *qkv/qkv* mice, the white matter of cerebellum was sparsely populated with EGFP-positive cells (Supplemental figure 1). No EGFP-positive cells were observed in the granule cell layer. There was no obvious difference between *qkv/qkv* and *w/qkv* littermates in the white matter near the deep cerebellar nuclei or in the white matter tracts (Supplemental Figure 1). Immunostaining for MBP revealed minimal signals in both groups,

as expected at P8. This suggests that prior to P8, the *qkv/qkv* cerebellum develops normally in terms of the arrival and generation of oligodendrocyte precursor cells (OPCs).

By P15, a large number of EGFP-positive cells were observed in the white matter (Figure 1A). At this stage we also detected a few PLP-EGFP+ cells in the granular layer of both *w/qkv* and *qkv/qkv* mice. Interestingly in the *qkv/qkv* cerebellum, a population of cells expressing very low levels of EGFP could be found in the granular and Purkinje layers (arrows in Figure 1B). Furthermore, in *w/qkv* cerebella, EGFP-expressing cells extended thin myelinating processes in the granular layer, as confirmed by the presence of MBP (Figure 1B). In comparison, *qkv/qkv* cerebella were found to express a much lower amount of myelinated segments (Figure 1B). The area per folia containing MBP fluorescence is 28.3 ± 8.6% and 5.4 ± 2.0% for *w/qkv* and *qkv/qkv*, respectively.

By P45 (young adult), an increase in the number of EGFP+ cells infiltrating the granular layer was observed in both wild-type and mutant mice, as compared to P15 (Figure 1C). However, *qkv/qkv* cerebella appear to have a much higher density of EGFP+ cells in both the proximal and distal white matter than that of *w/qkv* (Figure 1C). Myelination in the cerebellum is largely completed in the wild-type mouse by P45 (Foran and Peterson, 1992; Bouslama-Oueghlani et al., 2003). Consistently, we found that the myelinated segments appear uniform throughout the white matter and granular layer of *w/qkv* control mice (Figure 1D). However, in *qkv/qkv* littermates, MBP signals were much reduced and exhibited a fragmented pattern (Figure 1D, open arrowheads). The area per folia containing MBP fluorescence is 51.1 ± 7.5% and 31.6 ± 11.4% for *w/qkv* and *qkv/qkv*, respectively. We also observed discrete high-intensity MBP signals in *qkv/qkv* cerebella, which may correspond to redundant loops of non-compacted myelin (Bo et al., 1995; Gavino and Richard, 2011). The distribution of PLP-EGFP+ cells in P21 mice is similar to that of P45 with less MBP staining (Supplemental Figure 2). Therefore, the cerebellum of *qkv* mice appears to have altered oligodendroglial distribution and disrupted myelination.

To confirm that there was an increase in PLP-EGFP+ cells in various regions of the cerebellum of *qkv/qkv* mice, we counted the number of cells in different layers at P15. Cryosections were immuno-stained with calbindin antibody, which labels Purkinje cells, to identify the cerebellar layers (Figure 2A). PLP-EGFP+ cells were counted per unit area and normalized to the white matter tracts of *w/qkv* mice. We counted cells expressing both high and low levels of EGFP (Figure 2A). Although no significant difference in the number of PLP-EGFP+ was observed in either the white matter or molecular layers of *qkv/qkv* compared to *w/qkv* mice at P15 (Figure 2B), there were significant increases in the number of PLP-EGFP+ cells in the granular (control: 15.0 ± 6.4 versus *qkv*: 52.5 ± 14.4) and Purkinje layers (control: 3.4 ± 3.7 versus *qkv*: 72.4 ± 23.6). To determine whether these differences in cell number persist, we also quantified the number of PLP-EGFP+ cells in each of these layers in adult (P45) mice (Figure 2C). At P45, we continued to observe a significant increase in the density of PLP-EGFP+ cells in the granular layer (control: 18.8 ± 3.6 versus *qkv*: 160.1 ± 39.7), and Purkinje layer (control: 101.2 ± 0.6 versus *qkv*: 166.3 ± 18.1) of *qkv/qkv* compared to *w/qkv* littermates (Figure 2B). Moreover, we observed a significant increase in the density of PLP-EGFP+ cells in the white matter of P45 *qkv/qkv* mice (control: 100 ± 0 versus *qkv*: 375.1 ± 51.7) (Figure 2B), suggesting that the increase in

cell density in these mice continues into adulthood. Overall, this data suggests that the quakingviable mutation results in an increase as well as mislocalization of oligodendroglial cells within the cerebellum.

A recent study showed that overexpression of the Quaking isoforms, QKI-6 and QKI-7, can block the proliferation of myelinating Schwann cells (Larocque et al., 2009). To test if the loss of QKI in *qkv/qkv* mice could enhance cell proliferation leading to the increased number of PLP-EGFP-positive cells, we immunostained cryosections with the proliferation marker Ki67. In sections from P8 mice, Ki67+ cells were largely restricted to the external germinal layer, likely representing proliferating granule cells (Figure 3). Importantly, these cells were EGFP negative and we detected almost no individual PLP-EGFP+/Ki67+ cells in any region of the cerebellum in either *w/qkv* or *qkv/qkv* mice (Figure 3). In sections from P15 mice, we observed a marked decrease in the number of Ki67+ cells in the external granular layer and consistently no PLP-EGFP+/Ki67+ cells (Supplemental figure 3). It should also be noted that we did not observe any noticeable differences in the total number of Ki67+ cells at either age. It is known that cell proliferation in the adult cerebellum is extremely limited and our staining of P45 cerebellar cryosections showed no Ki67 signals for either *w/qkv* or *qkv/qkv* mice (data not shown). Together, these results suggest that the excess PLP-EGFP+ cells observed in *qkv/qkv* cerebella are unlikely a result of increased local oligodendroglial cell proliferation.

Therefore, we hypothesized that the increased number of PLP-EGFP+ cells in the cerebellar grey matter could be due to enhanced migration by these cells. To test this, we performed live imaging using organotypic cerebellar slice cultures prepared from P7 *qkv/qkv* and *w/qkv* littermate control mice every 72 hours for 12 days to track cell migration. Cell movement away from the white matter was quantified by dividing the cerebellum into three equal sized bins (based on the thickness of the white matter tract). Then the number of PLP-EGFP+ cells in each bin over time was counted and expressed as a percentage of the total number of cells. At day 1 in vitro (DIV 1, equivalent to ~P8), 87.9 ± 3.3% and 89.0 ± 3.6% (mean ± SD) of cells are located in bin 1, which represents the white matter, of *w/qkv* and *qkv/qkv* slices, respectively (Figure 4). However, as cells move outwards from the white matter, there is an increase in the percentage of cells residing in bins 2 and 3, which represents the grey matter. In control slices, while the number of cells in bin 2 steadily increases over time, the majority still remains in bin 1 by DIV 13 (~P20) (Figure 4). Very few PLP-EGFP+ cells are found in bin 3 (Bin 1: 66.5 ± 3.0% vs. Bin 2: 29.9 ± 1.1% vs. Bin 3: 2.1 ± 2.2%, mean ± SD). In contrast, PLP-EGFP+ cells from *qkv/qkv* slices have a higher percentage in bin 3, leading to a more homogenous distribution across the three bins by DIV 13 (Bin 1: 46.7 ± 4.3% vs. Bin 2: 32.1 ± 1.6% vs. Bin 3: 21.3 ± 4.1%, mean ± SD) (Figure 4). Thus, the higher number of PLP-EGFP+ cells in *qkv/qkv* mice may be a result of enhanced migration by OPCs.

As migrating bipolar OPCs differentiate into relatively stationary mature OLs, they extend a complex multi-polar network of branched processes. To quantify the number of migratory vs. stationary cells in *qkv/qkv* mice, we counted the number of PLP-EGFP+ cells with either a uni/bi-polar or multi-polar morphology (Figure 5). In *w/qkv* organotypic slices 60% of PLP-EGFP+ cells displayed a multipolar morphology at DIV1, with only 20% displaying a

bipolar morphology (Figure 5). By DIV 9 (~P16), 91.3% of cells displayed a multipolar morphology and only 8.7% remained bipolar. In *qkv/qkv* slices however, 26.7% of PLP-EGFP cells displayed a multipolar morphology at DIV1, with 73.3% displaying a non-polar or bipolar morphology. Furthermore, approximately 50% of EGFP+ cells retained their bipolar morphology, while 45.7% displayed a multipolar morphology at DIV 9 (Figure 5). This suggests that the enhanced migration of oligodendroglial cells in *qkv/qkv* mice is coupled to defects in cell differentiation that may lead to an increase in number of migratory OPCs.

One interesting observation in the *qkv/qkv* cerebellum is the dramatic increase in cells expressing relatively low levels of EGFP in the Purkinje and molecular layers (arrows in Figure 2). These low-expressing cells have long processes that extend from the Purkinje layer to the pial surface, reminiscent of Bergman glia. Therefore, we immunostained P15 cyrosections using the astrocytic marker GFAP. We found that the processes of most of the low-expressing EGFP+ cells in the Purkinje layer stained positively for GFAP, suggesting they are in fact Bergmann glia (Figure 6A). Although expression of the *Plp* gene is primarily restricted to oligodendroglial cells (Mallon et al., 2002), other cell types, such as neurons, have been found to also express PLP including neurons (Wang et al., 2009; Michalski et al., 2011). In addition, a recent study from Chung and colleagues found that while PLP+/Olig2+ NG2 precursor cells typically give rise to oligodendroglia in the cerebellum, they can also generate Bergmann glia (Chung et al., 2013). We similarly think that the low EGFP expressing cells in the Purkinje cell layer represent oligodendroglial precursors that have changed fate due to QKI downregulation. However, we cannot rule out the possibility that the QKI mutation simply induces the ectopic expression of EGFP under the PLP promoter in non-oligodendroglial lineage cells. When we examined both low and high EGFP-expressing cells in *qkv/qkv* mice, we found that the low-expressing cells in the Purkinje layer are GFAP + but Olig2−, while the relatively high-expressing cells throughout the white matter and granular layer are Olig2+ but GFAP− (Figure 6B & C). The majority of cells expressing moderate-to-high levels of EGFP within the white matter and granular layer stained positively for Olig2 (Figure 6C), suggesting that they are oligodendroglial lineage. This corresponds to our findings that approximately 90% of cells expressing high levels of EGFP in control *w/qkv* adult mice are Olig2+ (data not shown). Together, these results suggest that there are two distinct pools of PLP + cells in *qkv/qkv* mice, an Olig2+ pool and a GFAP+ pool, possibly with unique expression patterns and functions.

Discussion

Qkv mutant mice were first identified due to their severe hypomyelination of the CNS (Sidman et al., 1964). Since then, the QKI gene has been identified as an essential mediator of OL differentiation and myelination (Ebersole et al., 1996; Zhao et al., 2006; Chen et al., 2007). However, the exact cellular mechanisms leading to the hypomyelination of the CNS by QKI mutation remain to be fully understood. Moreover, little is known about QKI deficiency on oligodendrocyte development and myelination in cerebellum. In this study, we utilized imaging-based approaches to document the changes in oliogendroglial development in the cerebellum of *qkv/qkv* mice. We report that qkv mutation results in a sharp increase in migrating PLP-EGFP positive oligodendroglial cells, impairment of their differentiation and

myelin membrane production. We found that many of these PLP-EGFP-positive cells mislocalize to the cerebellar grey matter and maintain their bipolar morphology. Importantly QKI mutation results in the generation of two populations of PLP-EGFP-positive cells, one of which mislocalizes to the Purkinje layer to give rise to Bergmann glia. These findings suggest a role for QKI in the regulation of OPC differentiation, cell fate, and migration.

Interestingly, despite the overall increase in oligodendroglial cell migration, we did not observe any PLP-EGFP+ cells in the molecular layer of *qkv* mutant mice (Figure 4). Instead, the cells accumulated in the Purkinje layer where they gave rise to Bergmann glia, suggesting that something stopped them from migrating further. One possibility is that the OPCs were responsive to some cue from Purkinje cells or from cells in the molecular layer that altered their cell fate. This may be similar to what happens to Bergmann glia precursor cells. The cell bodies of normal Bergmann glia are found in the Purkinje layer where they form rosettes around each Purkinje cell (Reichenbach et al., 1995). The main processes of the Bergmann glia extend outwards into the molecular layer, terminating in end-feet at the sulci surface (Bellamy, 2006). They serve as guides for the migration of granule cells during early development (Hoogland and Kuhn, 2010). Early in vitro co-culture assays demonstrated that cerebellar neurons regulate astroglial differentiation, dramatically affecting their morphology and cell proliferation to produce Bergmann glia-like cells (Hatten, 1985; Nagata et al., 1986). More recently, several of the differentiation-promoting cues have been identified in cerebellar neurons. Among these, the release of Sonic hedgehog and FGF9 from Purkinje cells and granule cell precursors has been shown to induce Bergmann glia differentiation, respectively (Dahmane and Ruiz i Altaba, 1999; Lin et al., 2009). Bergmann glia are thought to derive from radial glial cells in the granular layer, however no intrinsic factors have been identified that regulate their subsequent differentiation thus far (Buffo and Rossi, 2013). Instead, it appears that Bergmann glia differentiation requires strict spatio-temporal regulation by the surrounding cerebellar milieu. It is interesting to consider whether the downregulation of QKI in PLP-EGFP+ oligodendroglia could somehow make them responsive to these extrinsic cues. On the other hand, PLP-EGFP+ cells could be responsive to these cues, however, under normal conditions they do not come into contact with them. It is only because of defects in cell differentiation in the *quakingviable* mice that these PLP-EGFP+ cells remain migratory for longer than usual and therefore receive these external signals. Finally, it is also important to note that QKI-5 and QKI-6 have previously been found expressed in Bergmann glia at levels comparable to OLs, although the localization pattern of QKI-5 differs between astrocytes and OLs (Hardy et al., 1996). This raises the alternative possibility that the formation of Bergmann glia requires the tight regulation of QKI in astrocyte precursors.

While PLP is an extremely abundant component of the myelin sheath, its expression can be observed early during postnatal development and is relatively dynamic. PLP expression is high in early progenitors, and then increases significantly during myelination (LeVine et al., 1990), as evidenced by intense EGFP signals in PLP-EGFP mice. However, we also observed cells expressing low levels of EGFP, mostly corresponding to GFAP+ Olig2− Bergmann glia. The low level of EGFP expression suggests that these cells were downregulating PLP expression. Interestingly, previous studies have shown that PLP-EGFP expression is not restricted to the oligodendrocyte lineage and can be found in both neurons

and astrocytes, suggesting that PLP-EGFP+ cells may function as multi-potential progenitor cells (Michalski et al., 2011; Harlow et al., 2014). It would be interesting to determine whether there are any changes in the number of specific progenitor populations in the absence of QKI. For example, is there an increase in the number of PLP-EGFP+ cells that stain for either or both of the early OPC progenitor markers, NG2 and PDGF-Rα, as might be expected given the change in cell morphology (e.g. increased bipolar or unipolar cell number), or for the neuronal marker NeuN? In this study, we were able to dramatically increase the number of PLP-EGFP+ Bergman glia via the downregulation of QKI. This raises the possibility that QKI downregulation can also induce the differentiation or transdifferentiation of PLP-EGFP+ cells into other cell types in the cerebellum, including neurons.

While the role of QKI in OL differentiation has been relatively well-studied, its function in regulating the cell cycle currently remains unclear. In OPCs and Schwann cells the overexpression of QKI-6 and QKI-7 has been shown to promote cell cycle arrest via the cyclin-dependent kinase inhibitor p27Kip1, a key regulator for cell cycle arrest (Larocque et al., 2005; Larocque et al., 2009). QKI binds to the p27Kip1 mRNA and stabilizes it, leading to increased accumulation of p27Kip1 protein in OPCs (Larocque et al., 2005). Previous studies had shown that overexpression of p27Kip1 can lead to cell cycle arrest of OPCs, whereas OPCs from p27Kip1 knockout mice show enhanced proliferation (Casaccia-Bonnefil et al., 1999; Tokumoto et al., 2002). However, knockdown of QKI in cultured CG4 oligodendrocyte precursor cells does not affect cell proliferation or cell cycle progression (Chen et al., 2007). Our findings in *qkv* mice suggest that QKI does not affect cell proliferation within the cerebellum. Instead, the increase in the number of oligodendroglia may be a result of enhanced migration. Alternatively, QKI downregulation could lead to a reduction in apoptosis of OPCs or a change in PLP-EGFP expression, thus contributing to the increase in the number of PLP-EGFP+ cells. Nonetheless, such an increase in OPCs may represent a mechanism by which the cerebellum attempts to compensate for the reduction in myelin in the *qkv* mouse by increasing the number of myelinating glial cells present.

Supplementary Material

Refer to Web version on PubMed Central for supplementary material.

Acknowledgement

This research was supported in part by grants from the National Institutes of Health to JQZ (GM083889 and MH104632), and YF (NS070526 and NS093016), and an F32 fellowship to KRM (NS092342).

References

Baumann N, Pham-Dinh D. Biology of oligodendrocyte and myelin in the mammalian central nervous system. Physiol Rev. 2001; 81:871–927. [PubMed: 11274346]

Bellamy TC. Interactions between Purkinje neurones and Bergmann glia. Cerebellum. 2006; 5:116–126. [PubMed: 16818386]

Bo L, Quarles RH, Fujita N, Bartoszewicz Z, Sato S, Trapp BD. Endocytic depletion of L-MAG from CNS myelin in quaking mice. J Cell Biol. 1995; 131:1811–1820. [PubMed: 8557747]

Bouslama-Oueghlani L, Wehrle R, Sotelo C, Dusart I. The developmental loss of the ability of Purkinje cells to regenerate their axons occurs in the absence of myelin: an in vitro model to prevent myelination. J Neurosci. 2003; 23:8318–8329. [PubMed: 12967994]

Buckner RL. The cerebellum and cognitive function: 25 years of insight from anatomy and neuroimaging. Neuron. 2013; 80:807–815. [PubMed: 24183029]

Buffo A, Rossi F. Origin, lineage and function of cerebellar glia. Prog Neurobiol. 2013; 109:42–63. [PubMed: 23981535]

Casaccia-Bonnefil P, Hardy RJ, Teng KK, Levine JM, Koff A, Chao MV. Loss of p27Kip1 function results in increased proliferative capacity of oligodendrocyte progenitors but unaltered timing of differentiation. Development. 1999; 126:4027–4037. [PubMed: 10457012]

Chen Y, Tian D, Ku L, Osterhout DJ, Feng Y. The selective RNA-binding protein quaking I (QKI) is necessary and sufficient for promoting oligodendroglia differentiation. J Biol Chem. 2007; 282:23553–23560. [PubMed: 17575274]

Chenard CA, Richard S. New implications for the QUAKING RNA binding protein in human disease. J Neurosci Res. 2008; 86:233–242. [PubMed: 17787018]

Chung SH, Guo F, Jiang P, Pleasure DE, Deng W. Olig2/Plp-positive progenitor cells give rise to Bergmann glia in the cerebellum. Cell Death Dis. 2013; 4:e546. [PubMed: 23492777]

Dahmane N, Ruiz i Altaba A. Sonic hedgehog regulates the growth and patterning of the cerebellum. Development. 1999; 126:3089–3100. [PubMed: 10375501]

Ebersole T, Rho O, Artzt K. The proximal end of mouse chromosome 17: new molecular markers identify a deletion associated with quakingviable. Genetics. 1992; 131:183–190. [PubMed: 1592235]

Ebersole TA, Chen Q, Justice MJ, Artzt K. The quaking gene product necessary in embryogenesis and myelination combines features of RNA binding and signal transduction proteins. Nat Genet. 1996; 12:260–265. [PubMed: 8589716]

Emery B. Regulation of oligodendrocyte differentiation and myelination. Science. 2010; 330:779–782. [PubMed: 21051629]

Eng LF, Chao FC, Gerstl B, Pratt D, Tavaststjerna MG. The maturation of human white matter myelin. Fractionation of the myelin membrane proteins. Biochemistry. 1968; 7:4455–4465. [PubMed: 5700665]

Foran DR, Peterson AC. Myelin acquisition in the central nervous system of the mouse revealed by an MBP-Lac Z transgene. J Neurosci. 1992; 12:4890–4897. [PubMed: 1281497]

Gavino C, Richard S. Loss of p53 in quaking viable mice leads to Purkinje cell defects and reduced survival. Sci Rep. 2011; 1:84. [PubMed: 22355603]

Hardy RJ, Loushin CL, Friedrich VL Jr, Chen Q, Ebersole TA, Lazzarini RA, Artzt K. Neural cell type-specific expression of QKI proteins is altered in quakingviable mutant mice. J Neurosci. 1996; 16:7941–7949. [PubMed: 8987822]

Harlow DE, Saul KE, Culp CM, Vesely EM, Macklin WB. Expression of proteolipid protein gene in spinal cord stem cells and early oligodendrocyte progenitor cells is dispensable for normal cell migration and myelination. J Neurosci. 2014; 34:1333–1343. [PubMed: 24453324]

Hatten ME. Neuronal regulation of astroglial morphology and proliferation in vitro. J Cell Biol. 1985; 100:384–396. [PubMed: 3881455]

Herrup K, Kuemerle B. The compartmentalization of the cerebellum. Annu Rev Neurosci. 1997; 20:61–90. [PubMed: 9056708]

Hoogland TM, Kuhn B. Recent developments in the understanding of astrocyte function in the cerebellum in vivo. Cerebellum. 2010; 9:264–271. [PubMed: 19904577]

Larocque D, Fragoso G, Huang J, Mushynski WE, Loignon M, Richard S, Almazan G. The QKI-6 and QKI-7 RNA binding proteins block proliferation and promote Schwann cell myelination. PLoS One. 2009; 4:e5867. [PubMed: 19517016]

Larocque D, Galarneau A, Liu HN, Scott M, Almazan G, Richard S. Protection of p27(Kip1) mRNA by quaking RNA binding proteins promotes oligodendrocyte differentiation. Nat Neurosci. 2005; 8:27–33. [PubMed: 15568022]

Larocque D, Pilotte J, Chen T, Cloutier F, Massie B, Pedraza L, Couture R, Lasko P, Almazan G, Richard S. Nuclear retention of MBP mRNAs in the quaking viable mice. Neuron. 2002; 36:815–829. [PubMed: 12467586]

LeVine SM, Wong D, Macklin WB. Developmental expression of proteolipid protein and DM20 mRNAs and proteins in the rat brain. Dev Neurosci. 1990; 12:235–250. [PubMed: 1705207]

Lin Y, Chen L, Lin C, Luo Y, Tsai RY, Wang F. Neuron-derived FGF9 is essential for scaffold formation of Bergmann radial fibers and migration of granule neurons in the cerebellum. Dev Biol. 2009; 329:44–54. [PubMed: 19232523]

Mallon BS, Shick HE, Kidd GJ, Macklin WB. Proteolipid promoter activity distinguishes two populations of NG2-positive cells throughout neonatal cortical development. J Neurosci. 2002; 22:876–885. [PubMed: 11826117]

Mecklenburg N, Garcia-Lopez R, Puelles E, Sotelo C, Martinez S. Cerebellar oligodendroglial cells have a mesencephalic origin. Glia. 2011; 59:1946–1957. [PubMed: 21901755]

Michalski JP, Anderson C, Beauvais A, De Repentigny Y, Kothary R. The proteolipid protein promoter drives expression outside of the oligodendrocyte lineage during embryonic and early postnatal development. PLoS One. 2011; 6:e19772. [PubMed: 21572962]

Nagata I, Keilhauer G, Schachner M. Neuronal influence on antigenic marker profile, cell shape and proliferation of cultured astrocytes obtained by microdissection of distinct layers from the early postnatal mouse cerebellum. Brain Res. 1986; 389:217–232. [PubMed: 3484997]

Nave KA. Myelination and support of axonal integrity by glia. Nature. 2010; 468:244–252. [PubMed: 21068833]

Reichenbach A, Siegel A, Rickmann M, Wolff JR, Noone D, Robinson SR. Distribution of Bergmann glial somata and processes: implications for function. J Hirnforsch. 1995; 36:509–517. [PubMed: 8568221]

Reynolds R, Wilkin GP. Development of macroglial cells in rat cerebellum. II. An in situ immunohistochemical study of oligodendroglial lineage from precursor to mature myelinating cell. Development. 1988; 102:409–425. [PubMed: 2458224]

Sidman RL, Dickie MM, Appel SH. MUTANT MICE (QUAKING AND JIMPY) WITH DEFICIENT MYELINATION IN THE CENTRAL NERVOUS SYSTEM. Science. 1964; 144:309–311. [PubMed: 14169723]

Sillitoe RV, Joyner AL. Morphology, molecular codes, and circuitry produce the three-dimensional complexity of the cerebellum. Annu Rev Cell Dev Biol. 2007; 23:549–577. [PubMed: 17506688]

Simons M, Misgeld T, Kerschensteiner M. A unified cell biological perspective on axon-myelin injury. J Cell Biol. 2014; 206:335–345. [PubMed: 25092654]

Tokumoto YM, Apperly JA, Gao FB, Raff MC. Posttranscriptional regulation of p18 and p27 Cdk inhibitor proteins and the timing of oligodendrocyte differentiation. Dev Biol. 2002; 245:224–234. [PubMed: 11969268]

Wang Y, Wu C, Caprariello AV, Somoza E, Zhu W, Wang C, Miller RH. In vivo quantification of myelin changes in the vertebrate nervous system. J Neurosci. 2009; 29:14663–14669. [PubMed: 19923299]

Zhang SC. Defining glial cells during CNS development. Nat Rev Neurosci. 2001; 2:840–843. [PubMed: 11715061]

Zhao L, Mandler MD, Yi H, Feng Y. Quaking I controls a unique cytoplasmic pathway that regulates alternative splicing of myelin-associated glycoprotein. Proc Natl Acad Sci U S A. 2010; 107:19061–19066. [PubMed: 20956316]

Zhao L, Tian D, Xia M, Macklin WB, Feng Y. Rescuing qkV dysmyelination by a single isoform of the selective RNA-binding protein QKI. J Neurosci. 2006; 26:11278–11286. [PubMed: 17079655]

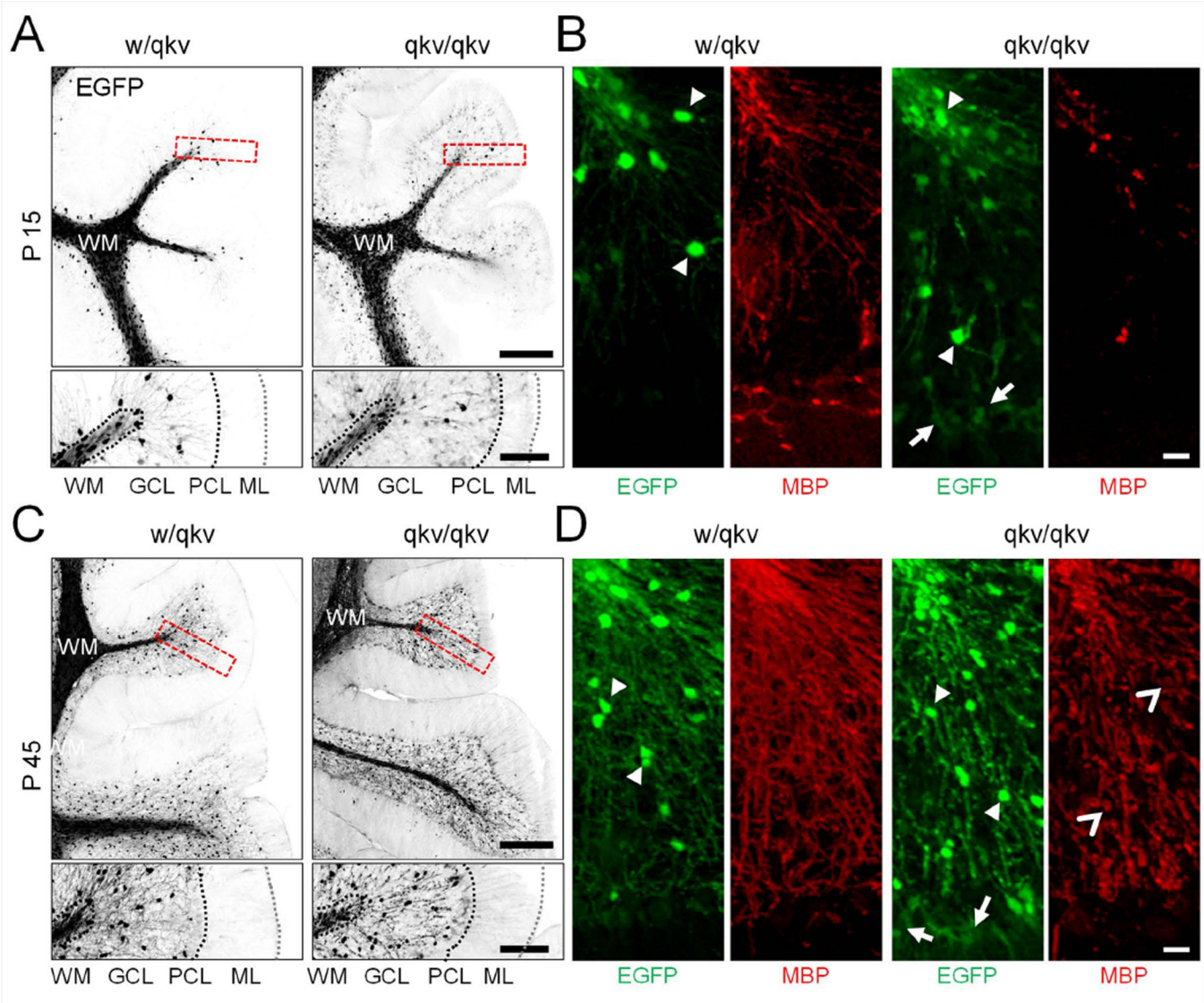

Figure 1.

PLP-EGFP+ cell distribution in the P15 and p45 cerebellum. (A,C) Top panels show representative images of sagittal cryosections from *w/qkv* and *qkv/qkv* littermates expressing PLP-EGFP at P15 and P45. Bottom panels are insets of boxed region from the end of single folium. (B,D) Images show EGFP+ cells (green) immunostained with anti-MBP (red) to detect myelin. Images represent maximum-intensity projections of at least 25 optical sections taken at 1 μm intervals stitched together. Arrowheads point to highly expressing EGFP+ cells, arrows point to weakly expressing EGFP+ cells, and open arrowheads point to fragmented regions of MBP staining. Scale bar (A,C) = 250 μm, insets = 100 μm; (B,D) = 20 μm.

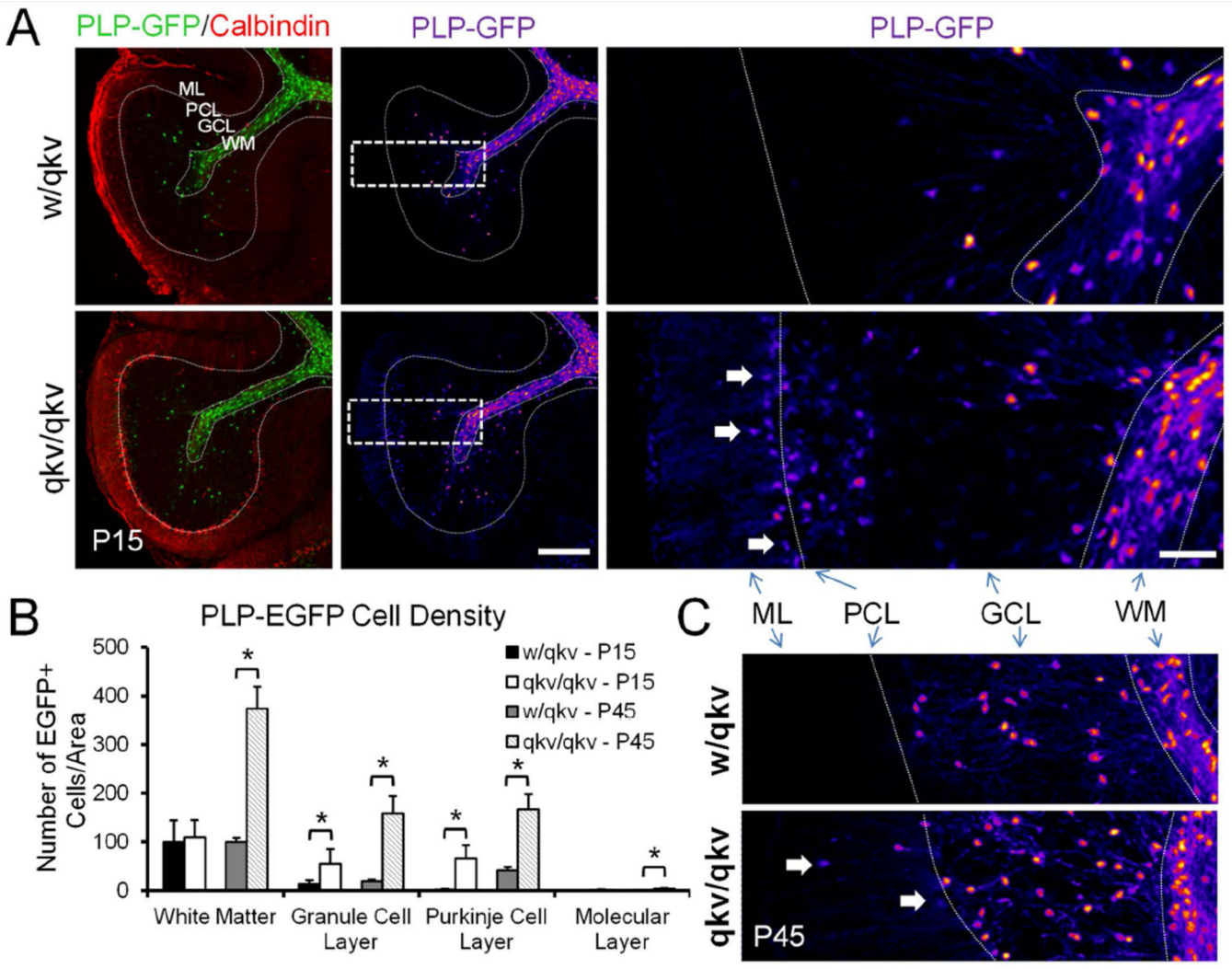

Figure 2.

Increased number of oligodendroglia in quakingviable mutant mice. (A) Left panels show sagittal cerebellar sections from P15 control *w/qkv* and *qkv/qkv* littermates expressing PLP-EGFP (green) immunostained with anti-Calbindin (red). Middle and right panels show PLP-EGFP cells pseudocolored to better visualize changes in fluorescence intensity due to cells expressing high and low levels of EGFP. Dashed rectangles in the middle panels indicate that regions that are shown in a higher magnification on the right. Cells expressing low levels of PLP-EGFP can be detected in the Purkinje and molecular layers of *qkv/qkv* mice. Scale bar = 200 μm, inset = 50 μm. (B) Histogram shows the average number of cells per unit area within each indicated region. Numbers are normalized to the number of cells per unit area in the white matter of control animals. Error bars: SD. *p<0.05 by Student's *t*-test. (C) Pseudocolored images of PLP-EGFP+ cells from P45 mice. WM=white matter, GCL=granule cell layer, PL=Purkinje layer, ML=Molecular layer.

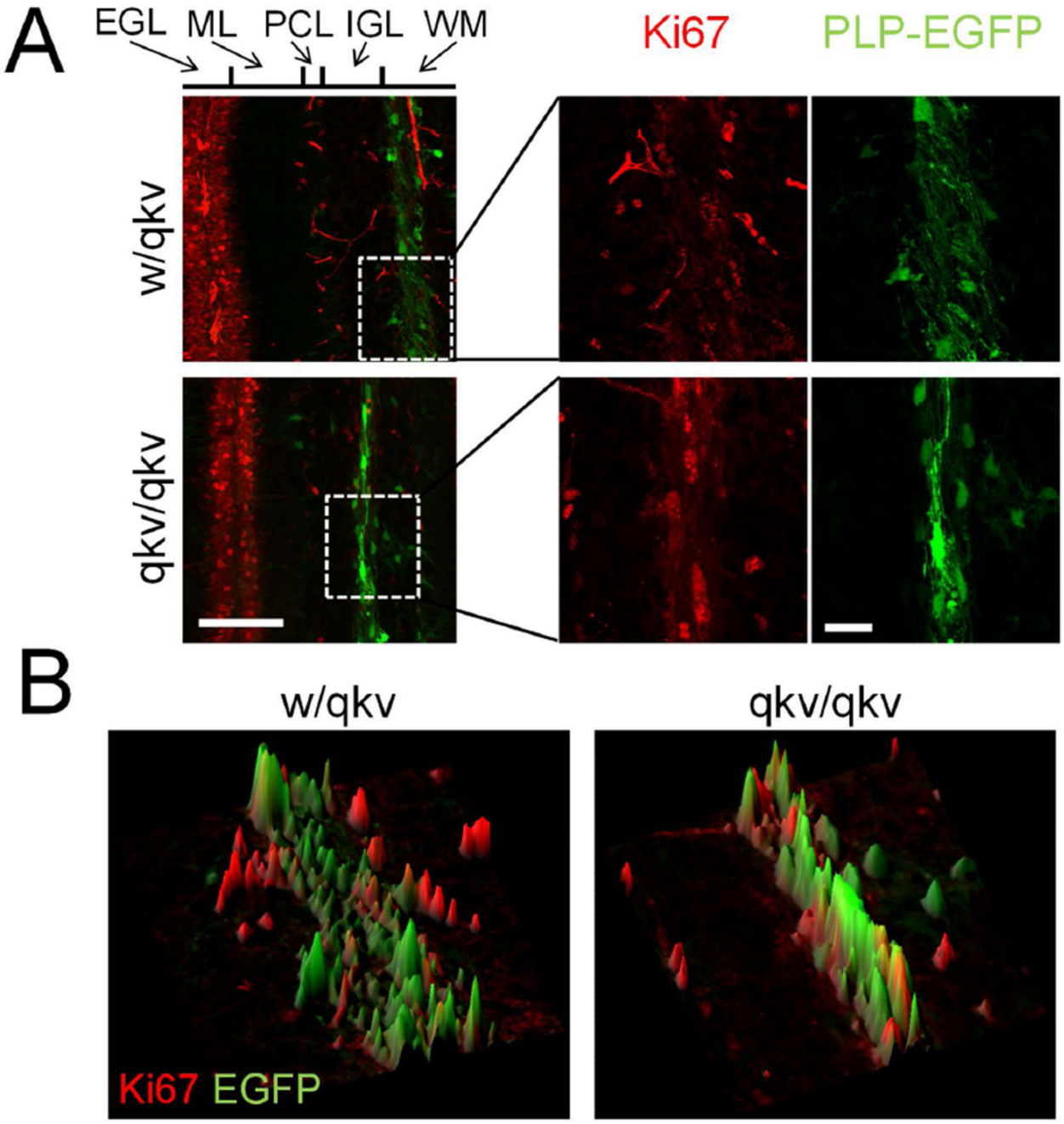

Figure 3.

Normal oligodendrocyte cell proliferation in *qkv* mice. (A) Ki67 staining (red) of P8 sagittal sections. Insets show magnification of boxed region. (B) 3D surface plots of insets from A illustrate the lack of overlap between EGFP+ and Ki67+ cells. Scale bars = 100 μm, inset = 25 μm.

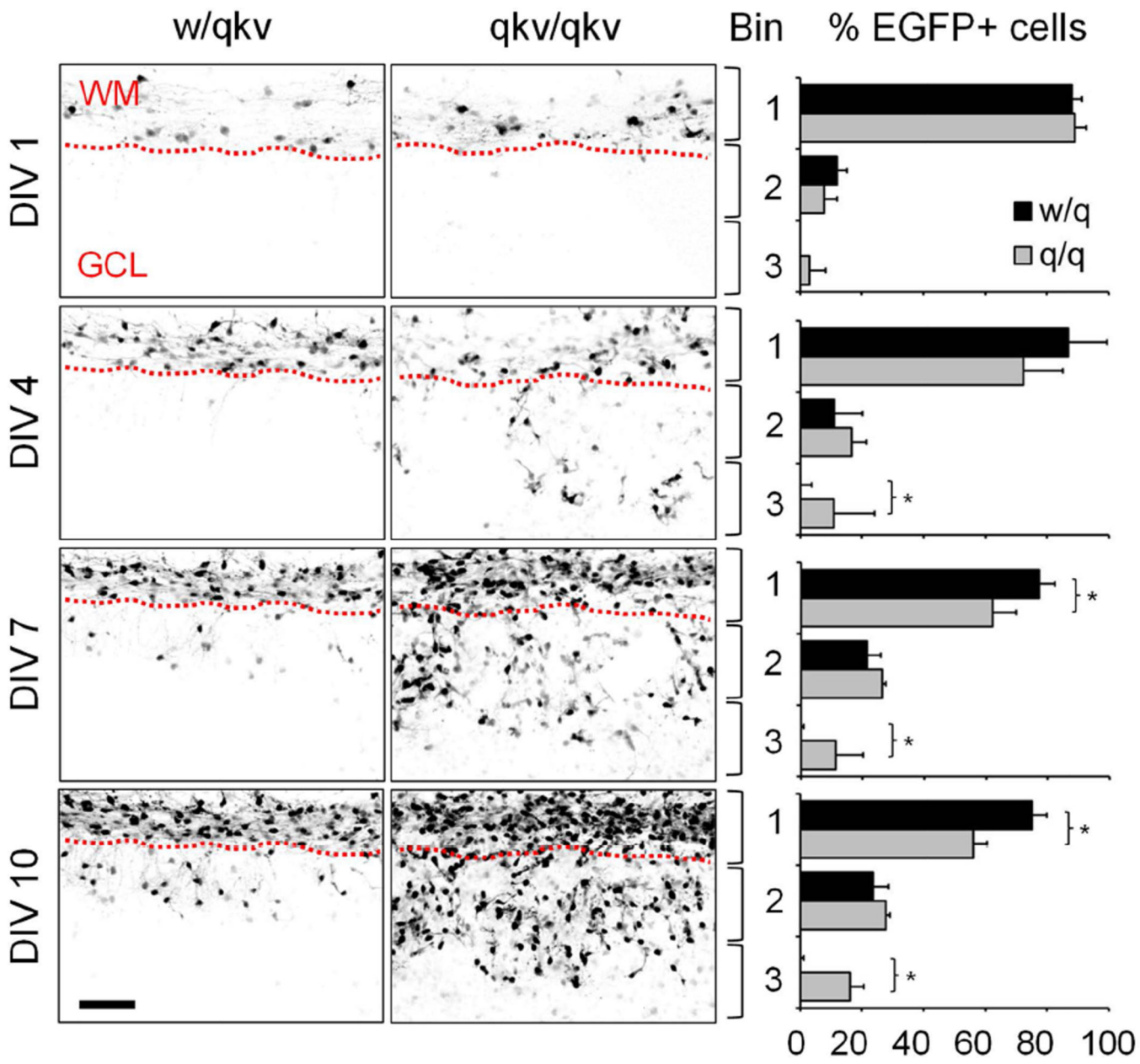

Figure 4.

Aberrant migration of oligodendroglia in *qkv* mice. Organotypic slice cultures were prepared from P7 heterozygous control (w/*qkv*) and quakingviable mutant (*qkv/qkv*) mice expressing PLP-EGFP. Images were acquired every 72 hours for 10 days, and represent maximum-intensity projections of at least 60 optical sections taken at 2 μm intervals. Histograms on right show the distribution of EGFP+ cells in each of three equivalent size bins expressed as a percentage of the total number of PLP-EGFP+ cells (n = 3 animals per genotype). Error bars: SD. *p<0.05 by Student's *t*-test. Scale bar = 100 μm. WM=white matter, GCL=granule cell layer.

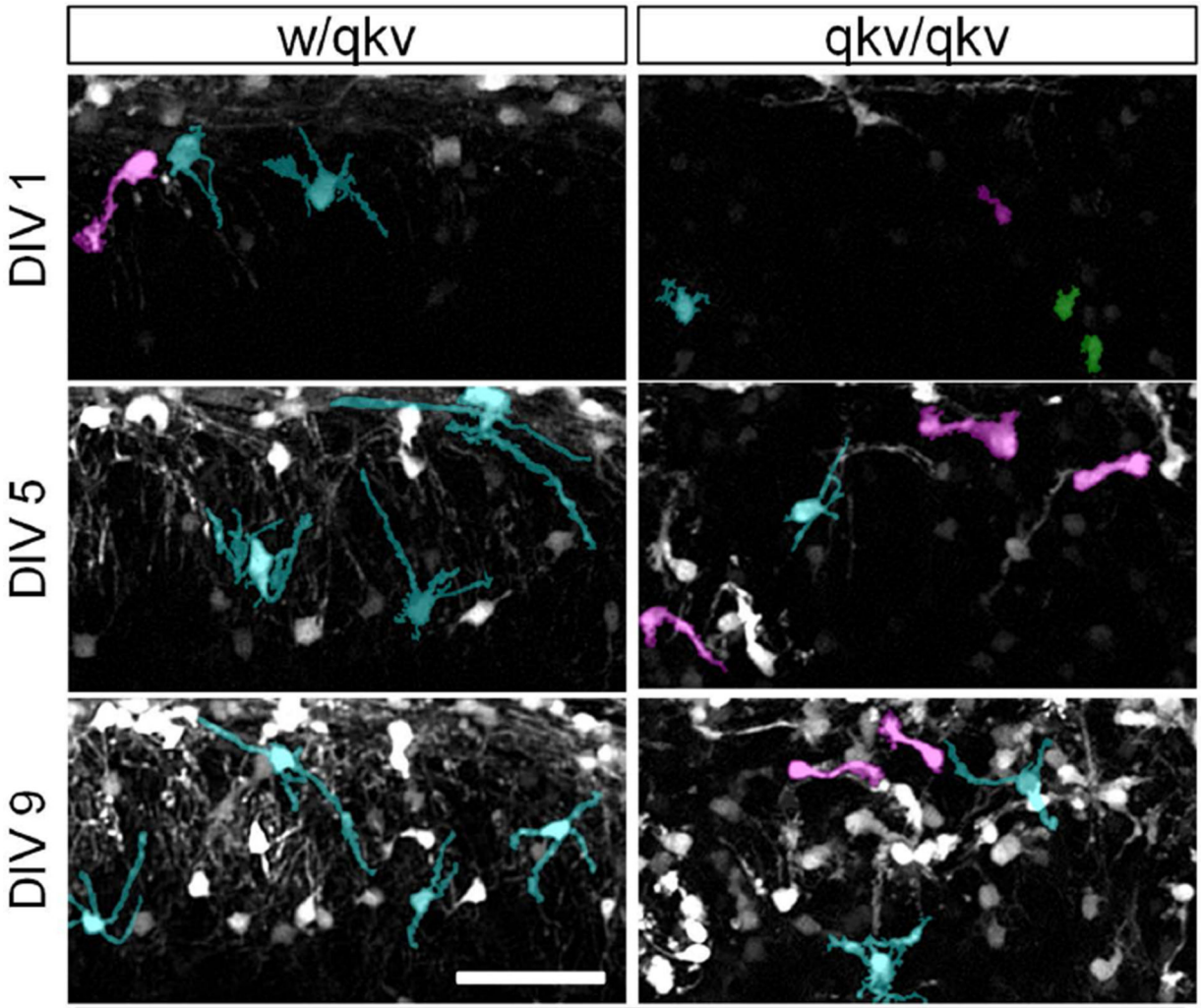

	DIV 1		DIV 5		DIV 9	
	w/q^v	q^v/q^v	w/q^v	q^v/q^v	w/q^v	q^v/q^v
Non-polar	20.0%	60.0%	0.0%	5.3%	0.0%	4.3%
Bi-polar	20.0%	13.3%	6.3%	73.7%	8.7%	50.0%
Multi-polar	60.0%	26.7%	93.8%	21.1%	91.3%	45.7%

Figure 5.

Many oligodendroglia in *qkv* mice retain migratory bipolar morphology. Organotypic cerebellar slice cultures were established from P8 heterozygous control (w/*qkv*) and quakingviable mutant (*qkv/qkv*) mice. Images represent maximum-intensity projections and were acquired 1, 5, and 9 days after plating. Individual representative cells in each panel were pseudo-colored to aid visualization of different cell morphologies as follows; green=non-polar, magenta=bi-polar, and cyan=multi-polar. Lower panel shows the percentage of cells with the indicated shapes at each age. Images shown are typical of

multiple regions within slices analyzed from at least 3 separate animals per genotype. Scale bar = 100 μm.

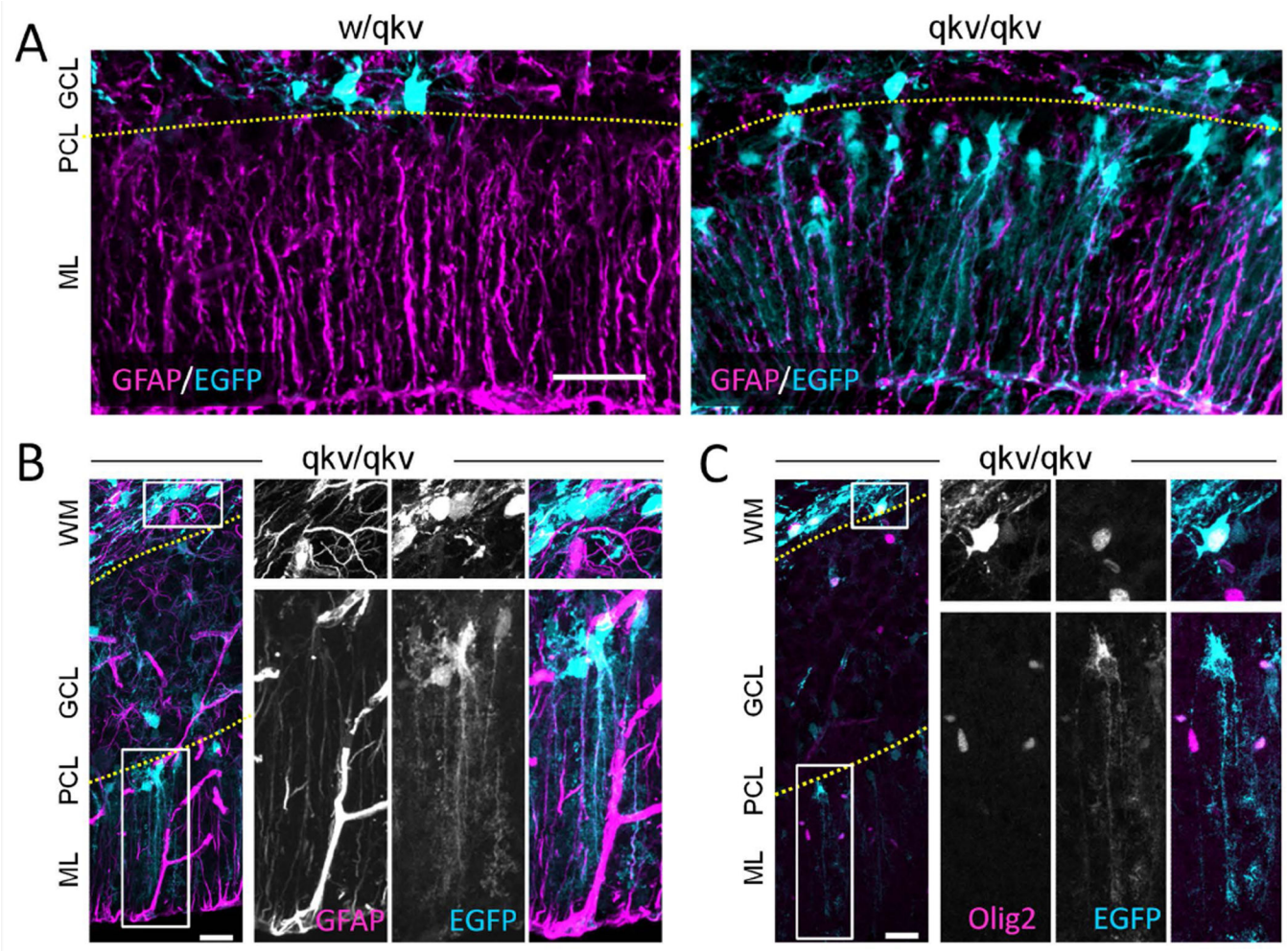

Figure 6.

PLP-EGFP+ cells in the Purkinje cell layer give rise to Bergmann glia in *qkv/qkv* mice. (A) Rrepresentative images of sagittal cerebellar section from P15 PLP-EGFP expressing (cyan) control w/qkv and *qkv/qkv* littermates stained with anti-GFAP antibody (magenta). (B–C) Representative panels show sagittal cerebellar sections from *qkv/qkv* mutant mice stained with anti-GFAP (B) or anti-Olig2 antibody (C), which are displayed in magenta whereas PLP-EGFP is shown in cyan. The boxed regions in WM and PCL are shown in 2X magnification on the right as individual channels (grayscale) and merged color image. The top panels on the right show the boxed region in WM of high PLP-GFP-expressing GFAP− cells (B) or high PLP-EGFP-expressing Olig2+ cells (C). The bottom panels on the right highlight the low PLP-EGFP-expressing GFAP+ cells (B) or low PLP-EGFP-expressing Olig2− cells (C) in PCL. Note that insets of low expressing EGFP+ cells were enhanced for visualization purposes. Scale bars (A) = 50 μm, (B–C) = 50 μm, insets = 12.5 μm. WM: white matter; GCL: granule cell layer; PCL: Purkinjie cell layer; ML: molecular layer. Yellow dotted lines indicate the layer separation.